Appl Biol Chem (2018) 61(2):197–208
https://doi.org/10.1007/s13765-018-0347-7

Online ISSN 2468-0842
Print ISSN 2468-0834

ARTICLE

Aqueous *Eucalyptus globulus* leaf extract-mediated biosynthesis of MgO nanorods

Jaison Jeevanandam[1] · Yen San Chan[1] · Yee Hung Ku[1]

Received: 20 December 2017 / Accepted: 14 January 2018 / Published online: 3 February 2018

Abstract Plant-based biosynthesis is gaining attention in nanoparticle synthesis as an alternate to chemical and physical synthesis routes due to their non-toxic and environment friendly nature. Leaf extract-based biosynthesis further facilitates rapid synthesis of non-toxic biocompatible nanoparticle that possesses various applications in biomedical and pharmaceutical industry. Metal oxides, especially MgO nanoparticles, show tremendous applications in medical industry. Moreover, plant-based biosynthesized MgO nanoparticles showed improved biophysical and biochemical properties. In the current study, MgO nanorods (MgONRs) are synthesized using *Eucalyptus globulus* aqueous leaf extract. The results are highly significant as rod-shaped nanoparticles possess superior cellular penetration ability than other morphologies and can be valuable in medical applications. A preliminary experiment was performed to identify the required reaction time for nanorod formation using dynamic light scattering technique. Later, one-factor-at-a-time approach was followed to identify the effect of each process parameters on average particle size of MgONRs. The optimized parameters were used for the synthesis of smaller-sized MgONRs. Fourier Transform infrared spectroscopy analysis was conducted to identify and analyze the functional groups in the leaf extract and MgONRs. The functional groups from phytochemicals and their transformation from enol to keto-form were found to be responsible for nanoparticle formation. The transmission electron microscope analysis showed that the optimized parameters yield 6–8 nm width of stacked MgONRs. Thus, the present work demonstrated a simple and rapid biosynthesis route for MgO nanorod synthesis which can be beneficial in biosensing and therapeutic application.

Keywords Biosynthesis · *Eucalyptus globulus* leaf extract · MgO nanorods · Phytochemicals

Introduction

Biosynthesis is an effective route to synthesize biocompatible metal oxide nanoparticles as it involves the usage of living organism that possess biological compounds for the production of nanoparticle [1]. Chemical and physical methods for nanoparticle synthesis are slowly to be replaced for biomedical applications due to their high cost and the tendency to create hazards to the environment and humans [2]. Among the biosynthesis methods, plant-mediated biosynthesis routes have showed a high promise in synthesizing nanoparticles, especially metal oxide nanoparticles [3]. However, the time required for nanoparticle synthesis is the major drawback in biological synthesis [3–5]. On the other hand, non-toxicity and environmental compatibility of plant leaf extracts make them as reliable biosynthesis agents for metal oxide nanoparticle synthesis [6]. Literatures also reported that the leaf extract-facilitated biosynthesis has improved bioactivity [7].

Among the metal oxides, magnesium oxide (MgO) possesses unique chemical inertness, optical transparency and secondary electron emission with high-temperature stability, high thermal conductivity [8–10] and toxic waste

✉ Yen San Chan
chanyensan@curtin.edu.my

[1] Department of Chemical Engineering, Faculty of Engineering and Science, Curtin University Malaysia, CDT 250, 98009 Miri, Sarawak, Malaysia

remediation ability [11–13]. Due to their distinctive properties, MgO in nano-form has been highly remarkable as catalysts and as absorbents [14, 15]. In biomedical application, there are evidential reports demonstrating MgO nanoparticle as an antibacterial agent [16, 17] and are used for the treatment of heartburn, cancer treatment and bone regeneration [18]. In the present study, *Eucalyptus globulus* was selected for MgO nanoparticle synthesis as it is commonly found in North Borneo region of Malaysia [19]. Eucalyptus oil [20] and phenols [21–23] are the major phytochemical components that are found in *E. globulus*. Besides, phytochemicals such as tannins, saponins, flavonoids, reducing sugars, glycosides and terpenoids that are essential in the bio-reduction of metal ions [24] are also present in the leaf extract of *E. globulus*.

Recently, Sharma and Jasuja [15] utilized *Swertia chirayaita* aqueous leaf extract in the synthesis of spherical MgO nanoparticles (< 20 nm) which showed significant antibacterial activity against several food and air borne bacteria [15]. Similarly, Jhansi et al. [25] used white button mushroom aqueous extract for the synthesis of spherical MgO nanoparticles (< 15 nm) which significantly increase the germination of *Arachis hypogaea L.* (peanut). Spherical-shaped MgO nanoparticles are also synthesized by using aqueous leaf extracts of *Pisidium guvajava*, *Aloe vera* [26], *Artemisia abrotanum* herb [27] and Arabic gum from Acacia trees [28]. Jeevanandam et al. [29] synthesized different sizes of MgO nanoparticles using several leaf extracts as well as magnesium precursors and investigated the effect of each synthesis parameters in yielding smaller-sized nanoparticles. Further, literature suggests that nanorods are suitable for biological applications such as biosensing, biomedical imaging, drug delivery and therapy [30] than other shapes. Recently, Karthik et al. [31] synthesized MgO nanorods (46 nm diameter) using *Andrographis paniculata* aqueous leaf extract which showed enhanced antibacterial and anti-breast cancer activity. It can be noted that the polyphenols such as epicatechin, quercetin-glucuronide [32] and flavonoids [33, 34] present in *E. globulus* help in transforming the shape of nanoparticles. Previous studies focused on synthesizing spherical-shaped, metal [35] and certain metal oxides such as iron oxides using *E. globulus* leaf extracts [36]. Therefore, the present work focuses on the biosynthesis of magnesium oxide nanorods (MgONRs) using *E. globulus* leaf extract as reducing and stabilizing agent. The main significance of the present work is the synthesis of smaller-sized (width), colloidal MgONRs at a shorter time period with the help of lower heat energy. Initially, dynamic light scattering (DLS) was used to sketch out the reaction time for the formation of MgONRs from magnesium ions. Later, one-factor-at-a-time (OFAT) approach was employed to optimize the synthesis parameters such as concentration of precursor, volume of leaf extract and reaction time to form smaller-sized MgONRs. The nature of MgONRs synthesized was analyzed by UV–visible absorbance spectroscopy, Fourier transform infrared spectroscopy (FTIR) analysis and transmission electron microscopy (TEM).

Materials and methods

Eucalyptus globulus leaves were purchased from the local market in Miri, Sarawak, Malaysia, while magnesium nitrate hexahydrate (98%) which served as the magnesium precursor was procured from Alfa Aesar® (Massachusetts, USA).

Preparation of leaf extract

Fresh leaves of *E. globulus* as shown in Fig. 1A were washed using distilled water to remove dirt and impurities. The cleaned leaves were placed in a bio-dryer (*BioSpec 1198 compact, 115VAC Bio-dryer*) until the leaves are completely dry and free from water. Then, the dried leaves were subsequently incised into smaller pieces and boiled with distilled water (1:9 ratio) for 20 min at 80 °C. The leaf extract was then filtered by using Whatman No.1 filter paper. The extracts as shown in Fig. 1B were stored in refrigerator for further use.

Synthesis of MgO nanorods

A total of 0.001 M of magnesium nitrate hexahydrate (precursor) was dissolved in 90 ml of distilled water. Then, 7% of aqueous leaf extract was slowly added dropwise into the solution with constant mixing for 20 min at 80 °C. The average size and PDI of the MgO nanoparticles were recorded for every 10 min for an hour using DLS technique to select the optimum reaction time for the formation of smaller-sized MgONRs via OFAT approach. The complete experimental procedure for the synthesis of MgONRs is depicted as a flowchart in Fig. 1C.

Characterization of MgO nanorods

Particle size distribution and polydispersity index of the samples were obtained by dynamic light scattering using *Malvern® Zetasizer Nano ZS*. Disposable folded capillary tube was used in which the sample was taken and the capillary tube was placed in the sample holder of the instrument. The analysis was performed by using backscattering of laser light at 173° angle with water as a dispersant. MgONRs prepared from the optimized parameters were characterized by using UV–visible absorbance spectroscopy, Fourier transform infrared (FTIR)

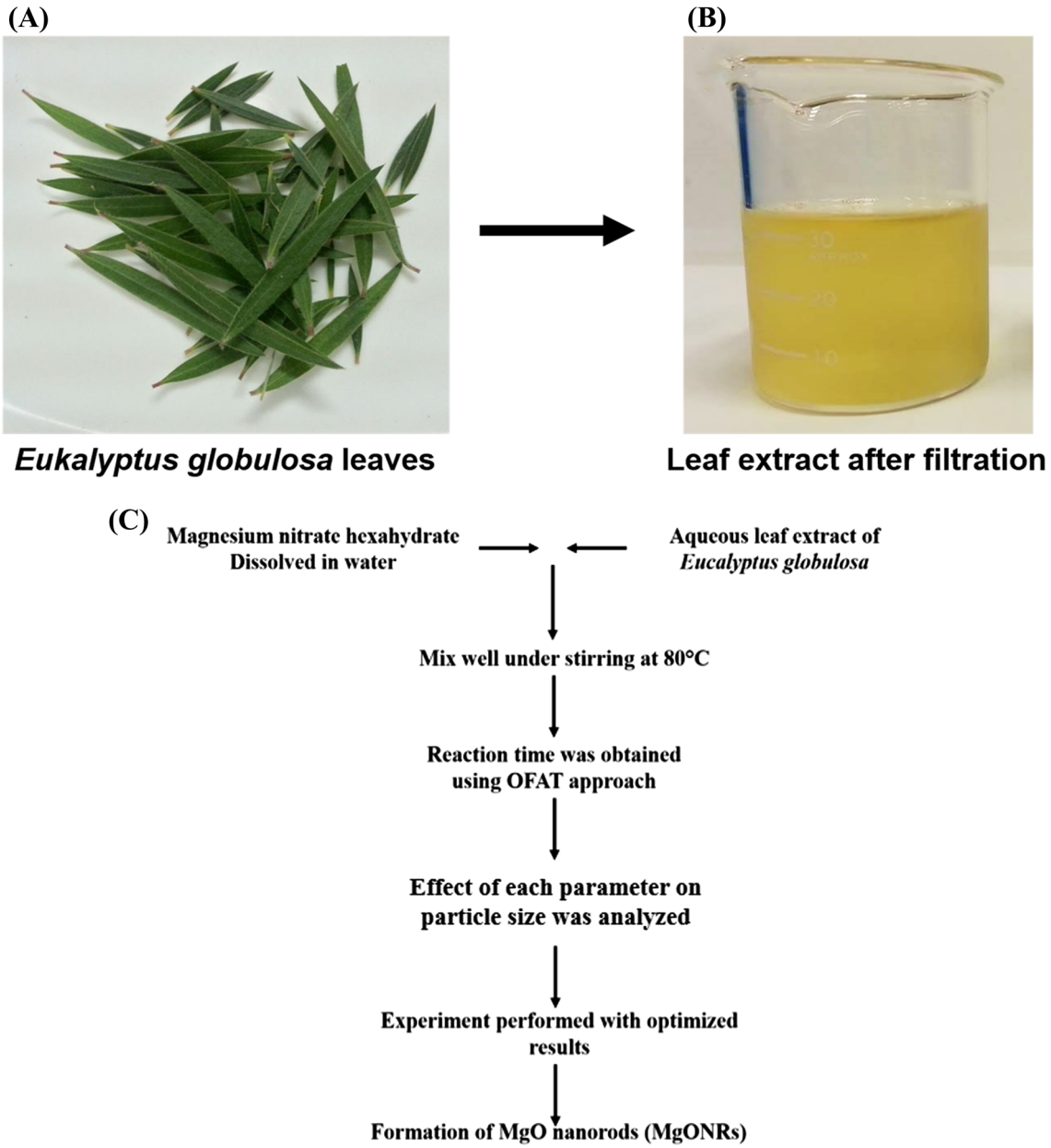

Fig. 1 (**A**) *Eucalyptus globulus* leaves, (**B**) *Eucalyptus globulus* leaf extract, (**C**) experimental flowchart for MgONRs synthesis

spectroscopy and TEM. *UV–Vis spectrophotometer Perkin Elmer® Lambda 25* was used to confirm the formation of metal oxide and to study the concentration of MgONRs formed in the sample. The sample was placed in a glass cuvette to analyze the absorbance of MgONRs from 800 to 300 nm wavelength. Fourier transform infrared spectroscopy *Thermo scientific NICOLET iS10* was used to identify the functional groups present in leaf extract and the synthesized MgONRs. A total of 250 mg of KBr was mixed with 1% of the sample and pelletized in a vacuum pelletizer which was scanned from a higher to lower (4000–500 cm^{-1}) wavenumber for the functional group analysis. *Tecnai^{TM} G^2 Spirit BioTWIN, FEI Company* TEM with 0.34 nm resolution was used to study the morphology of the nanorods. Briefly, the sample is suspended in water, coated on a 100-mesh copper grid, mounted on the TEM stage and is analyzed at 150,000× magnification to obtain clear images.

Results and discussion

UV–visible light absorbance studies

The reaction mixture containing aqueous leaf extract and magnesium precursor was mixed and heated as per the

experimental procedure in Fig. 1C. There is no visible color change to confirm the formation of MgO in the sample. Thus, UV–visible spectroscopy was used to confirm the presence of metal oxide. Mie theory states that the metal nanoparticles are conductors and their particle size is directly proportional to the light absorbance which leads to surface plasmon resonance [37]. However, metal oxide nanoparticles do not follow Mei theory as they are semiconductors with a gap between valence and conduction band [38]. This is the reason behind the usage of X-ray photoelectron spectroscopy to analyze metal oxide nanoparticles [39, 40]. The absorbance peak of MgO nanorod was obtained in the UV region (340 nm) [29, 41, 42] as mentioned in Fig. 2A. The inset in Fig. 2A shows another peak at 607 nm at absorbance below zero. This may be due to the light-reflecting behavior of metal oxide particles or due to light-absorbing phytochemicals which is difficult to detect and classify using UV–visible absorbance spectroscopy [43–45]. In spite of these drawbacks, UV–visible absorbance spectroscopy is a highly beneficial method for the preliminary confirmation of the presence of metal oxide nanoparticles. The peak at 340 nm confirms the presence of metal oxide nanoparticle, whereas the peak at 607 nm may also represent the presence of a rod-shaped particle. Huang and El-Sayed [46] revealed that UV–visible spectra split into two bands when the shape of nanoparticles changes from sphere to rod. This is due to the presence of nanorods that absorbs light at longer and shorter wavelength. The shorter wavelength represents the absorbance of light along the short axis of the nanorod, while the longer wavelength refers to the absorbance along the long axis of the nanorod [47]. The morphology analysis in Sect. 5 confirms that the shape of these particles is rod and the peak at 607 nm was due to rod shape of particles which was reduced either due to the interference of light-absorbing phytochemicals or light-reflecting nature of metal oxides.

One-factor-at-a-time (OFAT) approach

Once the presence of MgO was confirmed by UV–visible spectral analysis, DLS technique was used to identify the average size and PDI of the nanoparticle formed. The average particle size from the DLS technique was obtained from the light refracted by MgO present in the sample. Further, OFAT approach was used to determine the optimum reaction time for the MgONRs formation depending on the trend of average size and PDI. It is noted from Table 1 that the size of the nanorod was greatly affected by the reaction time. Recent studies by Nakaya et al. [48] and Dudhe et al. [49] revealed that the size of the nanoparticles can be controlled by optimizing the reaction time. Therefore, optimizing the reaction time is essential to decrease the size of nanoparticles and to prevent their agglomeration. Table 1 shows that the particle size obtained in 10 min of reaction time is 68.06 nm which decreased to 43.82 nm after 20 min. The PDI of particles until 60 min of the reaction time was below 0.6 due to their polydispersity, and the PDI of particles at 20 min of reaction time is 0.5 which is acceptable for a colloidal nanoparticle [50, 51]. Larger-particle-sized MgO was noted to be formed after 20 min of reaction time. Therefore, the optimum reaction time for the formation of MgONRs was found to be 20 min.

The proposed mechanism of MgO nanorod formation, based on the average size of the sample, is shown in Fig. 2B. It was deduced that the nucleation of nanorod formation starts at 10 min of reaction. Pacholski et al. [52] mentioned that increasing the heating time will help in elongation of the particle to form nanorods [52]. At 20 min

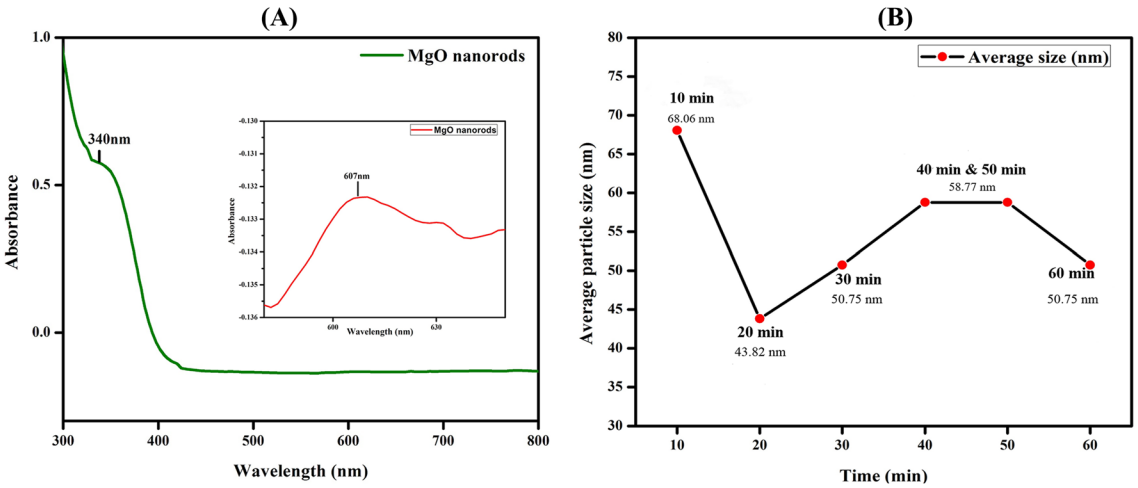

Fig. 2 (**A**) UV–visible absorbance of MgO nanorods from 300 to 800 nm; inset: UV–visible absorbance of MgO nanorods from 580 to 650 nm, (**B**) size transformation and mechanism of nanorod formation based on reaction time

Table 1 Average size and PDI of MgO nanoparticles formed at different reaction times

Time (min)	Average size (nm)	PDI
10	68.06	0.502
20	43.82	0.53
30	50.75	0.36
40	58.77	0.466
50	58.77	0.465
60	50.75	0.446

of reaction, the size of the nanoparticle drops down which may be due to the breakage of larger nucleated particles depending on the variables in process parameters. From 30 min of reaction time, the size of the nanoparticle starts to increase due to agglomeration of smaller particles to the larger surface of nanorods [53]. It is noted that the size of the nanorod drops at 60 min of reaction time can be attributed to the breakage larger nanorod after its threshold size and reaction time. Since, 20 min of reaction time yields smaller nanoparticles after nucleation, it was selected for further optimization of process parameters.

Effect of individual parameters on average particle size

An attempt has been made to analyze the effect of individual parameters on average particle size from the results obtained from DLS analysis through OFAT approach as mentioned in Table 2. Low, medium and high ranges of process parameters were selected for the analysis, and their effect on the average size of nanorods was discussed in detail.

Effect of precursor concentration

Precursor concentration is one of the determining factors for the synthesis of smaller-sized MgONRs. Sibiya et al. [54] reported that an increase in precursor concentration will help in effective capping ability that supports smaller nanoparticle formation. However, the average size of MgONRs is found to be increased from 50.75 to 91.28 with the increase in precursor concentration from 0.001 to 0.1 M. This may be due to the inability of phytochemicals as capping agent to control the nanoparticle size as the concentration of metal ions in the reaction mixture increases with an increase in precursor concentration [55]. Eventually, this leads to the agglomeration of nanoparticles through dipole–dipole interaction, and thus larger-sized nanoparticles are formed [55]. Amin et al. [56] reported that the precursor concentration controls the nucleation density. This evidence suggests that increasing precursor concentration may increase the number of nucleation sites and time for nanoparticle growth which leads to larger nanoparticle formation. Moreover, Abedini et al. [57] showed that the increase in precursor concentration will increase the number of ions which further leads to the increment in the collision probability of particle. Thus, lower precursor concentration will lead to smaller nanoparticle formation and helps in transforming its change along with other process parameters.

Effect of extract volume

Leaf extract volume also plays an important role in determining the average size of MgONRs. The leaf extract that possesses phytochemicals such as phenol, alkaloid, flavonoids, proteins, sugar and terpenoids has ability to reduce the precursor into metal ions [58]. The metal ions are then converted from mono or divert oxidation states to zero-valent states [58] which helps in the formation of nanoparticles. It was clear from the DLS analysis that the size of the nanorods decreased from 43.82 to 37.84 nm, when the volume of plant extract increased from 5 to 7 ml. This suggests that higher extract volume will increase the phytochemical quantity in the reaction mixture which effectively help in size reduction of MgONRs.

Effect of reaction time

The average size of the MgONRs can be noted to be smaller only at 20 min of reaction time compared to 15–25 min as mentioned in Table 2. The initial experiment to determine the time for nanorod formation also provides a

Table 2 Effect of individual parameters on average particle size

Process parameter	Low	Average particle size (nm)	Medium	Average particle size (nm)	High	Average particle size (nm)
Precursor concentration	0.001 M	50.75	0.05 M	68.06	0.1 M	91.28
Extract volume	3 ml	50.75	5 ml	43.82	7 ml	37. 84
Reaction time	15 min	50.75	20 min	43.82	25 min	78.82

similar result. This confirms that the size and shape determination of smaller MgONRs occurs in between 15 and 25 min of reaction time depending upon other process parameters. According to Ozel et al. [59], an increase in reaction time will result in rapid agglomeration of nanoparticles leading to increase in the size of nanoparticle. Similarly, Kotov [60] stated that prolonged reaction time may result in progressive decomposition of the stabilizing agent molecules that leads to the growth of nanocrystals. Thus, prolonged reaction time leads to crystal growth whereas short reaction time will not be sufficient for nucleation. Hence, an optimum (between 15 and 25 min) reaction time will help in forming smaller nanoparticle with modified shape. The effect of individual parameters in the formation of smaller MgONRs is depicted in Fig. 3A–C. Thus, the optimum parameters such as 0.001 M of precursor concentration, 7 ml of extract volume and 20 min of reaction time at 80 °C are selected to form smaller MgONRs.

Functional group analysis

Table 3 shows the functional groups present in the *E. globulus* aqueous leaf extract and chemical modifications due to the formation of MgONRs. The FTIR spectra of the leaf extract and MgONRs are presented in Fig. 4A.

The IR spectra of the leaf extract exhibit a strong and wide band at 3319.46 cm^{-1} and a short band at 1974.81 cm^{-1} which shifts to 3316.48 and 1982.02 cm^{-1}, respectively, in MgONRs. These bands are due to the O–H stretching vibrations which may be attributed to the presence of functional groups such as alcohol, carboxylic acid, ester and ether [61, 62]. According to Makarov et al. [1], flavonoids and phenols can transform from enol-form to keto-form which releases reactive hydrogen atom and form O–H group to reduce metal ions and form nanoparticles as shown in Fig. 3D, E. Literatures also suggested that higher content of total phenols in plant extracts possesses electron-donating ability to reduce the metal ions to form nanoparticles [63]. This shows that *E. globulus* leave extract contains phytochemicals that have O–H groups and the peak shift denotes a change due to the formation of MgONRs.

The peaks at 2162.46 and 2170.81 cm^{-1} in leaf extract and MgONRs, respectively, are due to the presence of –CΞC– vibration which is ascribed to the phytochemicals with alkyne functional group. The spectral band of the leaf extract at 1634 cm^{-1} is due to the presence of conjugated carbonyl (–C=O) vibration, and amino acid in phytochemicals is the major source of carbonyl functional group [64]. It can be observed that the nanorod formation did not affect the carbonyl group as there is no peak shift in the samples. In addition to this, Baskar et al. [65] argued that the peaks at 1538 and 1675 cm^{-1} are credited to the aromatic nitro compounds amides and open chain amino groups. Furthermore, Marutikesavakumar et al. [66] reported that the peak at 1636 cm^{-1} can be assigned for N–H bond of primary amines. Literature also shows the presence of amide I band at 1627 cm^{-1} and amide II band at 1650 cm^{-1} [67]. These amide I and II bands are formed due to the carboxyl stretch and N–H deformations in the amide linkages of the proteins [67]. Therefore, it was deduced that the MgONRs may be formed by utilizing free amine protein groups along with other phytochemicals. The carbonyl functional group which has strong binding ability with magnesium may act as a capping agent to avoid agglomeration of nanorods [68]. The Mg-O vibration peak at 400–800 cm^{-1} is absent in the MgONRs synthesized using aqueous leaf extract of *E. globulus*. However, recent literatures suggested that the peak at 1114.25–1414.21 cm^{-1} was due to the interaction of MgONRs in the network [69].

The functional group analysis confirms that the phytochemicals play an important role in the formation of nanoparticle by reducing the metal ions and helps in their subsequent stability. However, different plants have different concentration and composition of bioactive phytochemicals. It has been proposed that the size and morphology of nanoparticles are associated with interaction of these phytochemicals with the precursor [1]. Similarly, the shape and size of nanoparticles also depend on the experimental conditions such as temperature, precursor concentration, pH and the synthesis route (chemical, physical or biological). Studies by Khodashenas and Ghorbani [70] revealed that various shapes of nanoparticles can be prepared by adjusting the capping and reducing agent. The functional group analysis helps in identifying the probable bioactive phytochemicals that act as a reducing, stabilizing and capping agent for the formation of MgONRs.

Morphology analysis

Figure 4B, C shows the MgONRs synthesized by aqueous leaf extract of *E. globulus*. It can be observed that the width of nanorod ranges from 6 to 9 nm and the rods are stacked together. Literatures show that the stacking may be due to the van der Waals force of attraction between the particles due to their surface charge [71, 72]. The result is in agreement with the UV–visible spectroscopy analysis as Fig. 2A illustrates two absorption peaks indicating the nanorod formation. The size of the nanorod mentioned in TEM micrograph is different from the DLS analysis due to their spherical approximation of particles which is a major

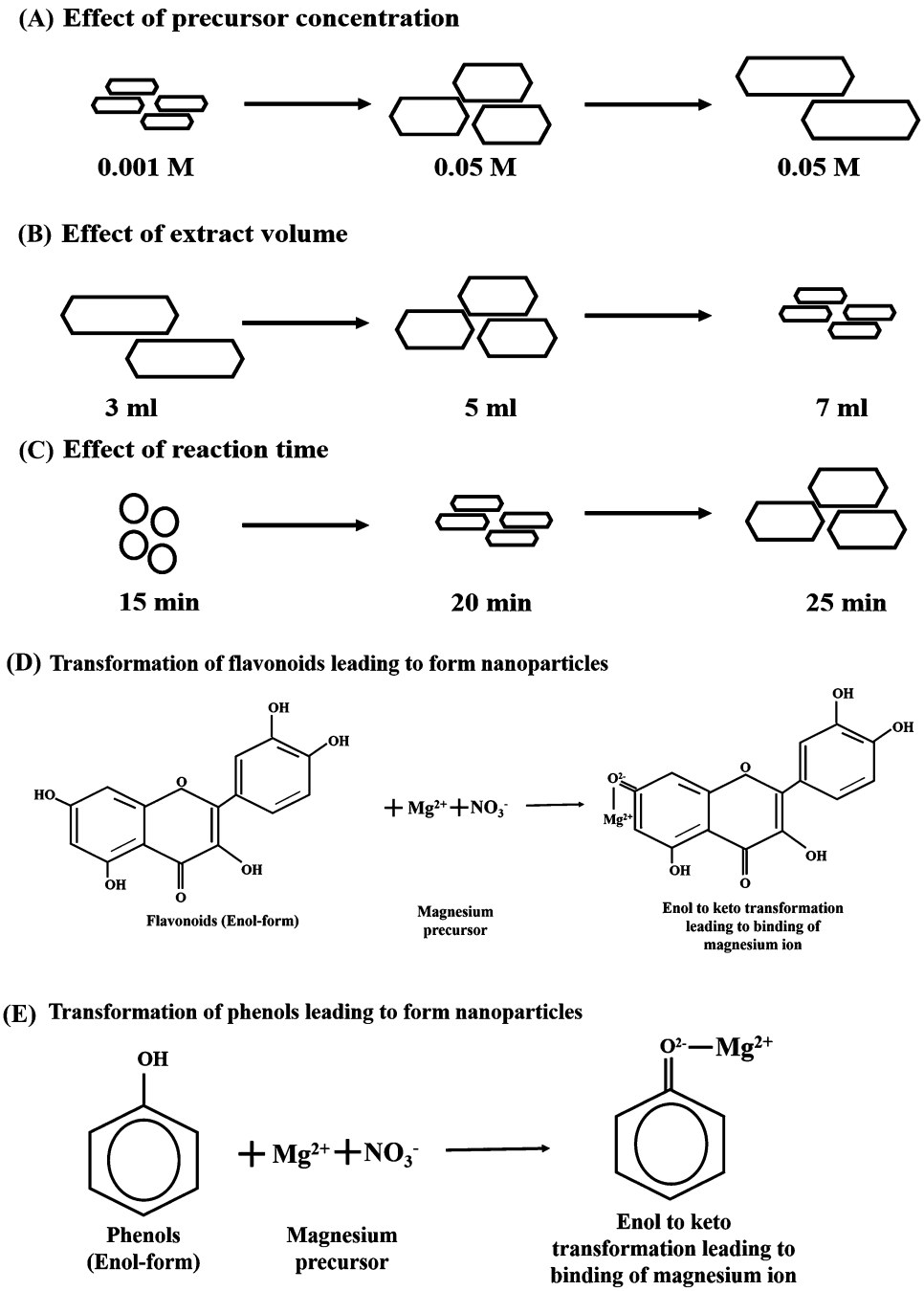

Fig. 3 Effect of (**A**) precursor concentration, (**B**) extract volume, (**C**) reaction time on size of the nanorods, transformation of enol- to keto-form of (**D**) flavonoids and (**E**) phenols leading to nanoparticle formation

Table 3 FTIR spectral chart showing functional groups in the leaf extract and MgO nanorods

Peak positions (cm^{-1})		Vibrational mode	Functional group
Leaf extract	MgO nanorods		
3319.46	3316.48	O–H stretch	Alcohol, carboxylic acid, ester, ether
2162.46	2170.81	–CΞC– stretch	Alkynes
1974.81	1982.02	C–O and C=O stretch	Alcohol, carboxylic acid, ester, ether
1634.36	1635.46	–C=O stretch or N–H bond	Carbonyl group, primary amine
–	1370.19	Mg-O	Magnesium oxide

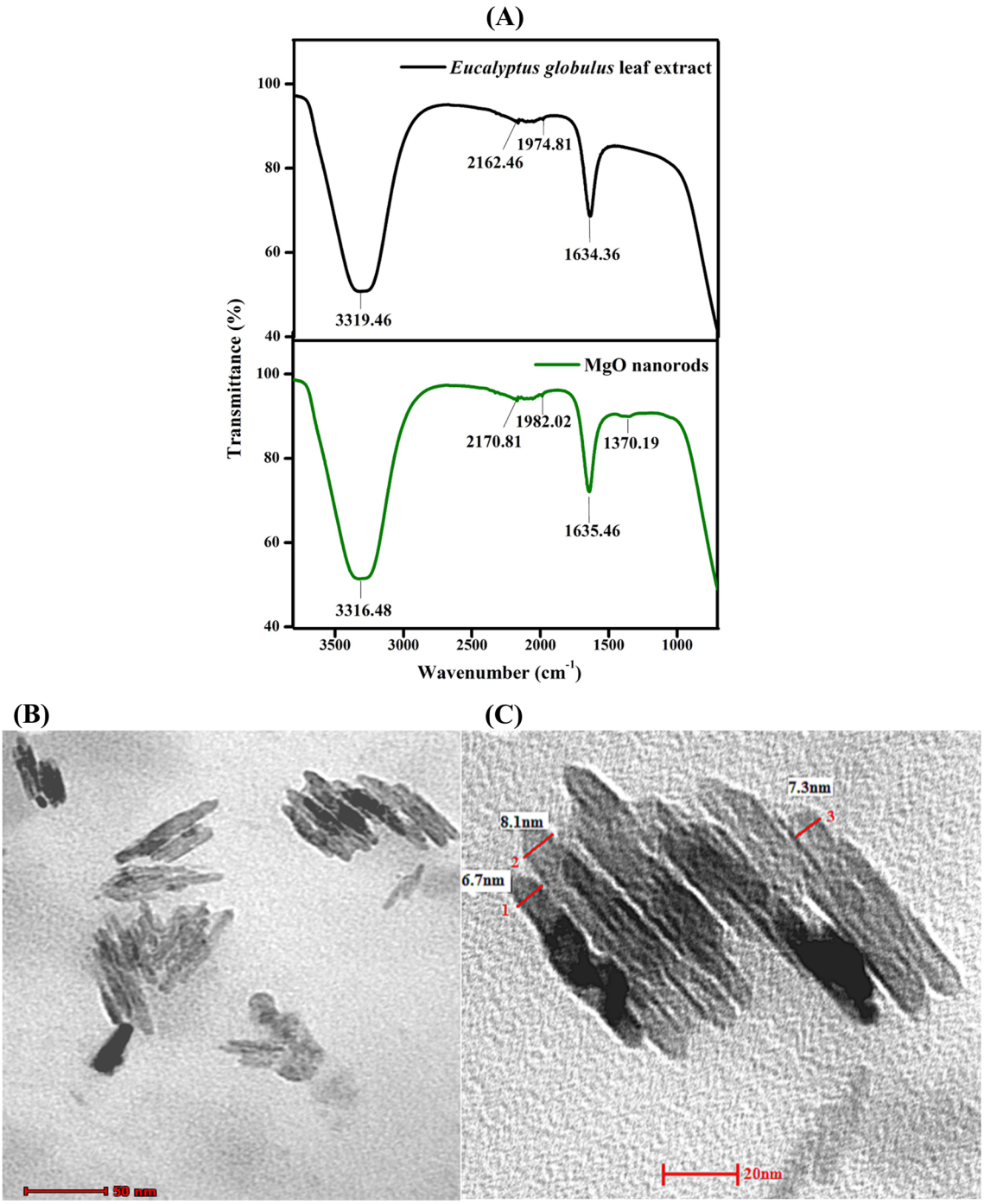

Fig. 4 (**A**) FTIR spectra of *Eucalytus globulus* leaf extract and MgO nanorods, TEM micrograph of MgO nanorods at (**B**) 50 nm scale and (**C**) 20 nm scale

drawback of DLS technique while analyzing rod-shaped particles [73, 74]. Literature suggested that high temperature and reaction time are essential for the formation of nanorods [75, 76]. The present study uses low temperature and reaction time along with phytochemicals as a reducing and stabilizing agent. Thus, the synthesized MgONRs are novel and will be highly biocompatible compared to other chemical synthesized MgO nanoparticles.

The possible mechanism for the formation of MgONRs is proposed in Fig. 5, based on the literature and from the results obtained from several characterization techniques in the present study. The major phytochemicals that are

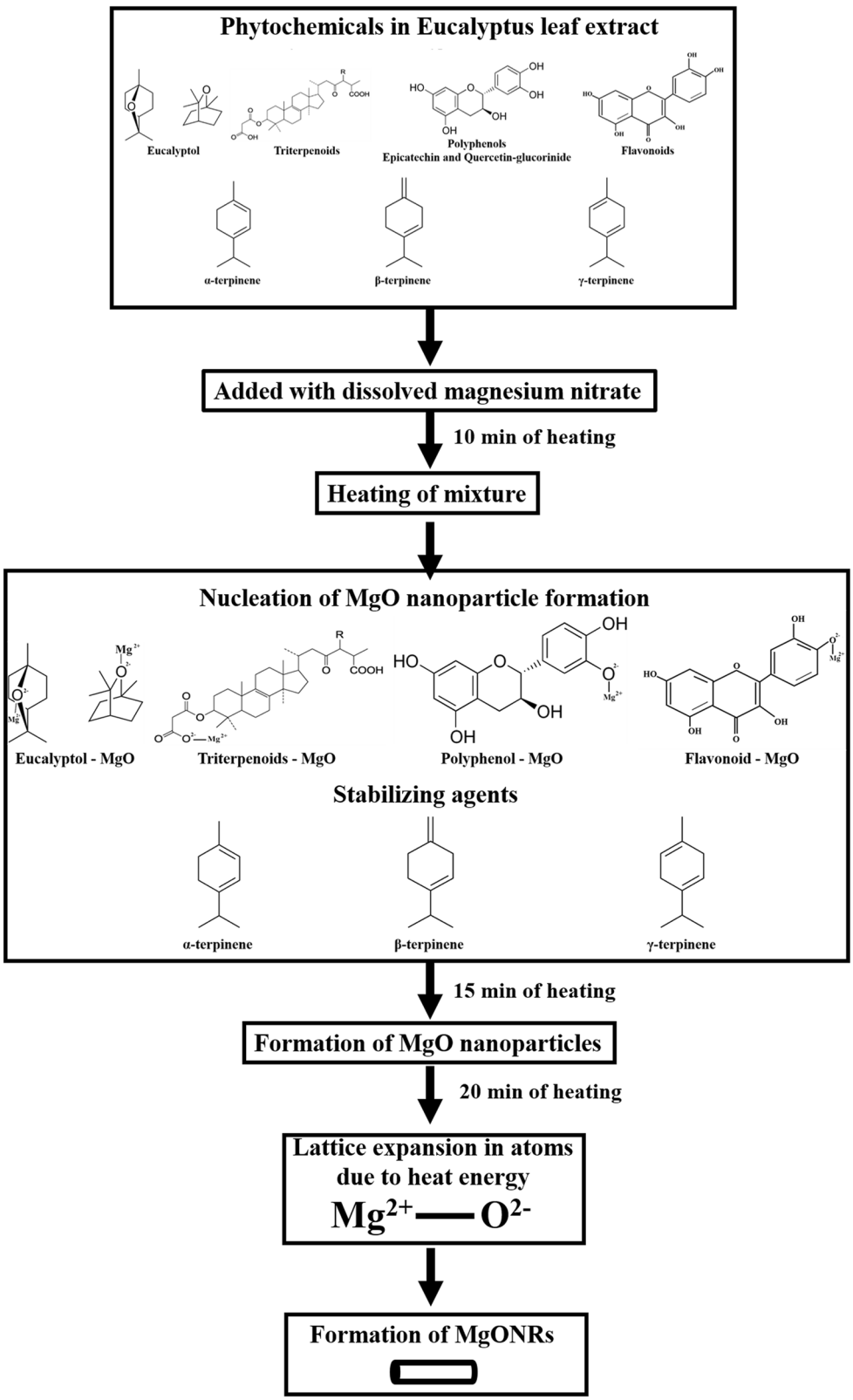

Fig. 5 Proposed mechanism for the formation of MgO nanorods

present in *E. globulus* leaf extracts are polyphenols, especially epicatechin and quercetin-glucuronide [32], eucalyptol, triterpenoids, terpinene [35] and flavonoids [77]. The aqueous crude leaf extract containing these phytochemicals was added to magnesium nitrate that is dissolved in distilled water. The mixture of phytochemicals and

dissolved magnesium nitrate was heated at 80 °C which leads to nucleation for nanoparticle formation as mentioned in the literature [78]. The phytochemicals absorb heat energy and transform into capping agent [79, 80] which makes it beneficial for the magnesium ions to bind with them for the nanoparticle formation. The phytochemicals such as eucalyptol, triterpenoids, polyphenols and flavonoids are predicted to be formed as a capping agent, whereas α-, β-, γ-terpinenes may act as the stabilizing agent for nanoparticle formation. This may be due to the lack of –OH group in terpinene which is an isomeric hydrocarbon phytochemical group [81]. After 15 min of heating process, MgO nanoparticles would have been formed which is evident from Fig. 2B. Further heating of the MgO nanoparticles (20 min) leads to the lattice expansion in atoms which expand in a linear direction due to phytochemical stabilizers [82] and form MgONRs. Thus, heat energy-based transformation of phytochemicals into the capping and gelling agent helps in the formation of MgONRs.

Among the morphologies, rod-shaped nanoparticles show attractive biological properties compared spherical shapes. Studies revealed that rod-shaped nanoparticles are highly potential in targeted drug delivery due to their large surface area and tendency to adhere effectively to the surface of the endothelial cells, allowing the drug to be delivered to the specific type of cells [83]. Despite this, it is not currently possible to draw conclusions about the influence of shape, as supportive data are still inadequate. Therefore, preliminary studies are still under investigation in order to explore the properties of non-spherical nanoparticles as drug delivery vectors. Khan et al. [84] reported that nanorods can be used as biomarkers as their large surface area may tend to modify with target molecules. Thus, the biocompatible MgONRs prepared using aqueous *E. globulus* leaf extract will be highly beneficial for biomedical applications.

Acknowledgments The authors would like to thank Curtin University, Malaysia, for the grant and facilities provided to support this work as well as UNIMAS, Sarawak, Malaysia, for the TEM testing facility.

References

1. Makarov VV, Love AJ, Sinitsyna OV, Makarova SS, Yaminsky IV, Taliansky ME, Kalinina NO (2014) "Green" nanotechnologies: synthesis of metal nanoparticles using plants. Acta Nat 6(1):35
2. Kharissova OV, Dias HR, Kharisov BI, Pérez BO, Pérez VMJ (2013) The greener synthesis of nanoparticles. Trends Biotechnol 31(4):240–248
3. Jeevanandam J, Chan YS, Danquah MK (2016) Biosynthesis of metal and metal oxide nanoparticles. ChemBioEng Rev 3(2):55–67
4. Mukherjee P, Ahmad A, Mandal D, Senapati S, Sainkar SR, Khan MI, Parishcha R, Ajaykumar P, Alam M, Kumar R (2001) Fungus-mediated synthesis of silver nanoparticles and their immobilization in the mycelial matrix: a novel biological approach to nanoparticle synthesis. Nano Lett 1(10):515–519
5. Narayanan KB, Sakthivel N (2010) Biological synthesis of metal nanoparticles by microbes. Adv Colloid Interface Sci 156(1):1–13
6. Prathna T, Mukherjee A, Raichur AM, Mathew L, Chandrasekaran N (2010) Biomimetic synthesis of nanoparticles: science, technology & applicability. INTECH Open Access Publisher, Rijeka
7. Bala N, Saha S, Chakraborty M, Maiti M, Das S, Basu R, Nandy P (2015) Green synthesis of zinc oxide nanoparticles using *Hibiscus sabdariffa* leaf extract: effect of temperature on synthesis, anti-bacterial activity and anti-diabetic activity. RSC Adv 5(7):4993–5003
8. Shukla S, Parashar G, Mishra A, Misra P, Yadav B, Shukla R, Bali L, Dubey G (2004) Nano-like magnesium oxide films and its significance in optical fiber humidity sensor. Sens Actuators B 98(1):5–11
9. Ma L, Lin Z, Lin J, Zhang Y, Hu L, Guo T (2009) Large-scale growth of ultrathin MgO nanowires and evaluate their field emission properties. Phys E (Amst Neth) 41(8):1500–1503
10. Badar N, Chayed N, Rusdi R, Kamarudin N, Kamarulzaman N (2011) Effect of annealing time on the morphology and particle size of magnesium oxide. Malays J Microsc 7(1):78–81
11. Copp A (1995) Magnesia/magnesite. Am Ceram Soc Bull 74(6):135–137
12. Wagner GW, Bartram PW, Koper O, Klabunde KJ (1999) Reactions of VX, GD, and HD with nanosize MgO. J Phys Chem B 103(16):3225–3228
13. Rajagopalan S, Koper O, Decker S, Klabunde KJ (2002) Nanocrystalline metal oxides as destructive adsorbents for organophosphorus compounds at ambient temperatures. Chem Eur J 8(11):2602–2607
14. Gesser H, Goswami P (1989) Aerogels and related porous materials. Chem Rev 89(4):765–788
15. Sharma G, Jasuja ND (2016) Phytoassisted synthesis of magnesium oxide nanoparticles by Swertia chirayaita. JTUSCI 11(3):471–477
16. Krishnamoorthy K, Manivannan G, Kim SJ, Jeyasubramanian K, Premanathan M (2012) Antibacterial activity of MgO nanoparticles based on lipid peroxidation by oxygen vacancy. J Nanopart Res 14(9):1–10
17. Leung YH, Ng A, Xu X, Shen Z, Gethings LA, Wong MT, Chan C, Guo MY, Ng YH, Djurišić AB (2014) Mechanisms of antibacterial activity of MgO: non-ROS mediated toxicity of MgO nanoparticles towards *Escherichia coli*. Small 10(6):1171–1183
18. Krishnamoorthy K, Moon JY, Hyun HB, Cho SK, Kim S-J (2012) Mechanistic investigation on the toxicity of MgO nanoparticles toward cancer cells. J Mater Chem 22(47):24610–24617
19. Salleh SB (1996) Eucalyptus plantations: the Malaysian experience. Reports submitted to the regional expert consultation on eucalyptus, vol II. FAO Regional Office for Asia and the Pacific, Bangkok, Thailand
20. Boland DJ, Brophy J, House A (1991) Eucalyptus leaf oils: use, chemistry, distillation and marketing. Inkata Press, Melbourne
21. Santos SA, Freire CS, Domingues MRM, Silvestre AJ, Neto CP (2011) Characterization of phenolic components in polar extracts of *Eucalyptus globulus* Labill. bark by high-performance liquid chromatography–mass spectrometry. J Agric Food Chem 59(17):9386–9393

22. Hou A-J, Liu Y-Z, Yang H, Lin Z-W, Sun H-D (2000) Hydrolyzable tannins and related polyphenols from *Eucalyptus globulus*. J Asian Nat Prod Res 2(3):205–212
23. Campos MG, Webby RF, Markham KR (2002) The unique occurrence of the flavone aglycone tricetin in Myrtaceae pollen. Zeitschrift für Naturforschung C 57(9–10):944–946
24. Godghate A, Sawant R (2014) Secondary metabolites determinations qualitatively from bark of *Butea monosperma* and *Eucalyptus globulus*. IJSET 3(2):497–501
25. Jhansi K, Jayarambabu N, Reddy KP, Reddy NM, Suvarna RP, Rao KV, Kumar VR, Rajendar V (2017) Biosynthesis of MgO nanoparticles using mushroom extract: effect on peanut (*Arachis hypogaea* L.) seed germination. 3 Biotech 7(4):263
26. Umaralikhan L, Jaffar MJM (2016) Green synthesis of MgO nanoparticles and it antibacterial activity. IJST Trans A. https://doi.org/10.1007/s40995-016-0041-8
27. Dobrucka R (2016) Synthesis of MgO Nanoparticles using *Artemisia abrotanum* Herba extract and their antioxidant and photocatalytic properties. IJST Trans A. https://doi.org/10.1007/s40995-016-0076-x
28. Fardood ST, Ramazani A, Joo SW (2018) Eco-friendly synthesis of magnesium oxide nanoparticles using arabic Gum. J. Appl. Chem. Res. 12(1):8–15
29. Jeevanandam J, Chan YS, Danquah MK (2017) Biosynthesis and characterization of MgO nanoparticles from plant extracts via induced molecular nucleation. New J Chem 41:2800–2814
30. Huang X, Neretina S, El Sayed MA (2009) Gold nanorods: from synthesis and properties to biological and biomedical applications. Adv Mater 21(48):4880–4910
31. Karthik K, Dhanuskodi S, Gobinath C, Sivaramakrishnan S (2017) Microwave assisted green synthesis of MgO nanorods and their antibacterial and anti-breast cancer activities. Mater Lett 206:217–220
32. Santos SA, Villaverde JJ, Freire CS, Domingues MRM, Neto CP, Silvestre AJ (2012) Phenolic composition and antioxidant activity of *Eucalyptus grandis*, *E. urograndis* (*E. grandis* × *E. urophylla*) and *E. maidenii* bark extracts. Ind Crops Prod 39:120–127
33. Sheny D, Mathew J, Philip D (2012) Synthesis characterization and catalytic action of hexagonal gold nanoparticles using essential oils extracted from *Anacardium occidentale*. Spectrochim Acta Part A 97:306–310
34. Raghunandan D, Basavaraja S, Mahesh B, Balaji S, Manjunath S, Venkataraman A (2009) Biosynthesis of stable polyshaped gold nanoparticles from microwave-exposed aqueous extracellular anti-malignant guava (*Psidium guajava*) leaf extract. NanoBiotechnology 5(1–4):34–41
35. Ali K, Ahmed B, Dwivedi S, Saquib Q, Al-Khedhairy AA, Musarrat J (2015) Microwave accelerated green synthesis of stable silver nanoparticles with *Eucalyptus globulus* leaf extract and their antibacterial and antibiofilm activity on clinical isolates. PLoS ONE 10(7):e0131178
36. Balamurugan M, Saravanan S, Soga T (2014) Synthesis of iron oxide nanoparticles by using *Eucalyptus globulus* plant extract. e-J Surf Sci Nanotechnol 12:363–367
37. Kelly KL, Coronado E, Zhao LL, Schatz GC (2003) The optical properties of metal nanoparticles: the influence of size, shape, and dielectric environment. J Phys Chem B 107(3):668–677
38. Nicollian EH, Brews JR, Nicollian EH (1982) MOS (metal oxide semiconductor) physics and technology, vol 1987. Wiley, New York
39. Lanje AS, Sharma SJ, Pode RB, Ningthoujam RS (2010) Synthesis and optical characterization of copper oxide nanoparticles. Adv Appl Sci Res 1(2):36–40
40. Bora T, Lakshman KK, Sarkar S, Makhal A, Sardar S, Pal SK, Dutta J (2013) Modulation of defect-mediated energy transfer from ZnO nanoparticles for the photocatalytic degradation of bilirubin. Beilstein J Nanotechnol 4(1):714–725
41. Alwan RM, Kadhim QA, Sahan KM, Ali RA, Mahdi RJ, Kassim NA, Jassim AN (2015) Synthesis of Zinc oxide nanoparticles via sol-gel route and their characterization. Nanosci Nanotechnol 5(1):1–6
42. Umar AA, Rahman MYA, Taslim R, Salleh MM, Oyama M (2011) A simple route to vertical array of quasi-1D ZnO nanofilms on FTO surfaces: 1D-crystal growth of nanoseeds under ammonia-assisted hydrolysis process. Nanoscale Res Lett 6(1):1
43. Klaas J, Schulz-Ekloff G, Jaeger NI (1997) UV-visible diffuse reflectance spectroscopy of zeolite-hosted mononuclear titanium oxide species. J Phys Chem B 101(8):1305–1311
44. Morales AE, Mora ES, Pal U (2007) Use of diffuse reflectance spectroscopy for optical characterization of un-supported nanostructures. Rev Mex Fis S 53(5):18
45. Dacome AS, Da Silva CC, Da Costa CE, Fontana JD, Adelmann J, Da Costa SC (2005) Sweet diterpenic glycosides balance of a new cultivar of *Stevia rebaudiana* (Bert.) Bertoni: isolation and quantitative distribution by chromatographic, spectroscopic, and electrophoretic methods. Process Biochem (Oxford, UK) 40(11):3587–3594
46. Huang X, El-Sayed MA (2010) Gold nanoparticles: optical properties and implementations in cancer diagnosis and photothermal therapy. J Adv Res 1(1):13–28
47. Sabatini DM (2007) Leading edge nanotechnology research developments. Nova Publishers, Hauppauge, New York
48. Nakaya M, Nishida R, Muramatsu A (2014) Size control of magnetite nanoparticles in excess ligands as a function of reaction temperature and time. Molecules 19:11395–11403
49. Dudhe C, Nagdeote S (2014) Effect of reaction rate and calcination time on $CaNb_2O_6$ nanoparticles. J Nanosci 909267:5
50. ISO13321 I (1996) Methods for determination of particle size distribution part 8: photon correlation spectroscopy. International Organisation for Standardisation (ISO)
51. Gaumet M, Vargas A, Gurny R, Delie F (2008) Nanoparticles for drug delivery: the need for precision in reporting particle size parameters. Eur J Pharm Biopharm 69(1):1–9
52. Pacholski C, Kornowski A, Weller H (2002) Self-assembly of ZnO: from nanodots to nanorods. Angew Chem Int Ed 41(7):1188–1191
53. Ahn S, Kim K, Chun Y, Yoon K (2007) Nucleation and growth of Cu (In, Ga) Se 2 nanoparticles in low temperature colloidal process. Thin Solid Films 515(7):4036–4040
54. Sibiya PN, Xaba T, Moloto MJ (2016) Green synthetic approach for starch capped silver nanoparticles and their antibacterial activity. Pure Appl Chem 88(1–2):61–69
55. Sibiya PN, Moloto MJ (2014) Effect of precursor concentration and pH on the shape and size of starch capped silver selenide nanoparticles. Chalcogenide Lett 11(11):577–588
56. Amin G, Asif MH, Zainelabdin A, Zaman S, Nur O, Willander M (2011) Influence of pH, precursor concentration, growth time, and temperature on the morphology of ZnO nanostructures grown by the hydrothermal method. J Nanomater 2011:9
57. Abedini A, Daud AR, Abdul Hamid MA, Kamil Othman N, Saion E (2013) A review on radiation-induced nucleation and growth of colloidal metallic nanoparticles. Nanoscale Res Lett 8(1):474
58. Shah M, Fawcett D, Sharma S, Tripathy SK, Poinern GEJ (2015) Green synthesis of metallic nanoparticles via biological entities. Materials 8(8):7278–7308
59. Ozel F, Kockar H, Karaagac O (2015) Growth of iron oxide nanoparticles by hydrothermal process: effect of reaction parameters on the nanoparticle size. J Supercond Novel Magn 28(3):823–829

60. Kotov NA (2005) Nanoparticle assemblies and superstructures. CRC Press, Cambridge
61. Khan M, Naqvi AH, Ahmad M (2015) Comparative study of the cytotoxic and genotoxic potentials of zinc oxide and titanium dioxide nanoparticles. Toxicol Rep 2:765–774
62. Li J, Barron AR (2010) Fourier transform infrared spectroscopy of metal ligand complexes. OpenStax-CNX module: m3 4660
63. Abdel-Aziz MS, Shaheen MS, El-Nekeety AA, Abdel-Wahhab MA (2014) Antioxidant and antibacterial activity of silver nanoparticles biosynthesized using *Chenopodium murale* leaf extract. J Saudi Chem Soc 18(4):356–363
64. Geethalakshmi R, Sarada D (2010) Synthesis of plant-mediated silver nanoparticles using *Trianthema decandra* extract and evaluation of their anti microbial activities. Int J Eng Sci Res Technol 2(5):970–975
65. Baskar G, Chandhuru J, Fahad KS, Praveen A (2013) Mycological synthesis, characterization and antifungal activity of zinc oxide nanoparticles. AJP Technol 3(4):142–146
66. Marutikesavakumar C, Yugandhar P, Savithramma N (2015) Adansonia digitata leaf extract mediated synthesis of silver nanoparticles; characterization and antimicrobial studies. J Appl Pharm Sci 5(8):082–089
67. Ismail EH, Khalil MM, Al Seif FA, El-Magdoub F (2014) Biosynthesis of gold nanoparticles using extract of grape (*Vitis vinifera*) leaves and seeds. Prog Nanotechnol Nanomater 3:1–12
68. Kim Y-W, Boyer R (2015) Microstructure/property relationships in titanium aluminides and alloys: proceedings of the seven session symposium on" microstructure/property ralationships in titanium alloys and titanium aluminides," Sponsored by the titanium committee of the minerals, metals and materials society held at the 1990 TMS Fall Meeting, Detroit, Michigan, 7–11 October 1990. Tms
69. Asgharzadehahmadi SA (2012) Synthesis and characterization of polyacrylamide based hydrogel containing magnesium oxide nanoparticles for antibacterial applications. Universiti Teknologi Malaysia, Johor Bahru
70. Khodashenas B, Ghorbani HR (2015) Synthesis of silver nanoparticles with different shapes. Arab J Chem (In Press)
71. Almeida M, Cavalcante L, Li MS, Varela JA, Longo E (2012) Structural refinement and photoluminescence properties of MnWO4 nanorods obtained by microwave-hydrothermal synthesis. J Inorg Organomet Polym Mater 22(1):264–271
72. Gopannagari M, Kumar DP, Reddy DA, Hong S, Song MI, Kim TK (2017) In situ preparation of few-layered WS 2 nanosheets and exfoliation into bilayers on CdS nanorods for ultrafast charge carrier migrations toward enhanced photocatalytic hydrogen production. J Catal 351:153–160
73. Gigault J, Mignard E, El Hadri H, Grassl B (2017) Measurement bias on nanoparticle size characterization by asymmetric flow field-flow fractionation using dynamic light-scattering detection. Chromatographia 80(2):287–294
74. Pecora R (2000) Dynamic light scattering measurement of nanometer particles in liquids. J Nanopart Res 2(2):123–131
75. Zijlstra P, Bullen C, Chon JW, Gu M (2006) High-temperature seedless synthesis of gold nanorods. J Phys Chem B 110(39):19315–19318
76. Kalpana D, Han JH, Park WS, Lee SM, Wahab R, Lee YS (2014) Green biosynthesis of silver nanoparticles using Torreya nucifera and their antibacterial activity. Arab J Chem (In Press)
77. Takahashi T, Kokubo R, Sakaino M (2004) Antimicrobial activities of eucalyptus leaf extracts and flavonoids from *Eucalyptus maculata*. Lett Appl Microbiol 39(1):60–64
78. Saleem S, Ahmed B, Khan MS, Al-Shaeri M, Musarrat J (2017) Inhibition of growth and biofilm formation of clinical bacterial isolates by NiO nanoparticles synthesized from *Eucalyptus globulus* plants. Microb Pathog 111:375–387
79. Wang T, Jin X, Chen Z, Megharaj M, Naidu R (2014) Green synthesis of Fe nanoparticles using eucalyptus leaf extracts for treatment of eutrophic wastewater. Sci Total Environ 466:210–213
80. Wang T, Lin J, Chen Z, Megharaj M, Naidu R (2014) Green synthesized iron nanoparticles by green tea and eucalyptus leaves extracts used for removal of nitrate in aqueous solution. J Clean Prod 83:413–419
81. Ott J, Gronemann V, Pontzen F, Fiedler E, Grossmann G, Kersebohm D, Weiss G, Witte C (2012) Ullmann's encyclopedia of industrial chemistry. Wiley-VCH, Weinheim
82. Robinson RD, Sadtler B, Demchenko DO, Erdonmez CK, Wang L-W, Alivisatos AP (2007) Spontaneous superlattice formation in nanorods through partial cation exchange. Science 317(5836):355–358
83. Truong NP, Whittaker MR, Mak CW, Davis TP (2015) The importance of nanoparticle shape in cancer drug delivery. Expert Opin Drug Deliv 12(1):129–142
84. Khan A, Rashid R, Murtaza G, Zahra A (2014) Gold nanoparticles: synthesis and applications in drug delivery. Trop J Pharm Res 13(7):1169–1177